PRAMANA
— journal of
physics

Vol. 59, No. 2
August 2002
pp. 385–395

Wave attenuation model for dephasing and measurement of conditional times

A M JAYANNAVAR and COLIN BENJAMIN
Institute of Physics, Sachivalaya Marg, Bhubaneswar 751 005, India

Abstract. Inelastic scattering induces dephasing in mesoscopic systems. An analysis of previous models to simulate inelastic scattering in such systems is presented and a relatively new model based on wave attenuation is introduced. The problem of Aharonov–Bohm (AB) oscillations in conductance of a mesoscopic ring is studied. We show that the conductance is symmetric under flux reversal and the visibility of AB oscillations decays to zero as a function of the incoherence parameter, signaling dephasing. Further the wave attenuation model is applied to a fundamental problem in quantum mechanics, that of the conditional (reflection/transmission) times spent in a given region of space by a quantum particle before scattering off from that region.

Keywords. Electron transport; dephasing; sojourn times; wave attenuation.

PACS Nos 72.10.-d; 73.23.-b; 05.60.Gg; 85.35.Ds; 03.65.-w; 03.65.Xp; 42.25.Bs.

1. Introduction

We present a study of two different problems in mesoscopic physics which are of current interest, namely, dephasing and other conditional times. This work considers these two phenomena not from a microscopic point of view but through a phenomenological model which captures the essence of these quite well. The model is known as the wave attenuation model. It essentially involves damping the wave function in the region of interest, so as to derive essential physics. In the context of dephasing, we consider an Aharonov–Bohm (AB) interferometer, and show that the wave attenuation model is better than its counterpart the optical potential model used in this context. Also, in case of double heterostructures we employ this technique to clock the time a particle takes to traverse a local region of interest in the given system. Here also the wave attenuation model is simpler to deal with than other models.

2. Dephasing

The process of dephasing or decoherence leads to the diminishing of quantum effects or loss of quantum mechanical interference effects. Dephasing occurs due to interaction of an electron (interfering entity) with its environmental degrees of freedom (which are not measured in the interference experiment) [1,2]. The AB oscillations are one of the prime

examples for analyzing how quantum interference effects are affected by dephasing. These oscillations are similar to the fringes seen in a Young's double slit experiment apart from the presence of the magnetic flux. In the Young's double slit interferometer the intensity is given by $I = |\Psi|^2 = |\psi_1|^2 + |\psi_2|^2 + 2\Re(\psi_1^* \psi_2 e^{i\phi})$, where ψ_1 and ψ_2 are the complex wave amplitudes across the upper and lower arms of the interferometer and ϕ is the phase difference between these two wave amplitudes, and the part $2\Re(\psi_1^* \psi_2 e^{i\phi})$ represents the interference term. If there is no steady phase relationship between the waves, the average intensity will be $\langle I \rangle = |\psi_1|^2 + |\psi_2|^2$. Complete dephasing is indicated by extinction of these interference terms. Thus, dephasing can be defined as a phenomenon because of which quantum mechanical systems behave as though they are described by classical probability theory.

2.1 *Models for dephasing*

In the absence of a complete microscopic theory as to how inelastic scattering affects dephasing, models are useful. There are different ways to model dephasing in mesoscopic systems. An interesting method is to attach a voltage probe [3] to the sample as in the inset of figure 1 (Buttiker's model). In this model, an electron captured by a voltage probe is injected back with an uncorrelated phase leading to irreversible loss of phase memory. This model has built-in current conservation, and Onsager's symmetry relations are obeyed, but it does suffer from a major demerit in that it only describes localized dephasing.

The optical potential model provides another method of introducing dephasing in these mesoscopic samples. The optical potential was first introduced to explain the inelastic cross-section in case of neutron scattering. In this model a spatially uniform optical potential $(-iV_i)$ is added to the Hamiltonian [4], making it non-hermitian. This leads to removal of particles from phase coherent motion. While absorption is real in the case of photons there is no absorption for electrons. The absorption of electrons is reinterpreted [5] as scattering into other energy levels and therefore proper re-injection is necessary. Zohta and Ezawa [4] interpreted that the total transmission after re-injection is defined as the sum of two contributions, one due to the coherent part and the other due to the incoherent part, i.e., $T_{\rm tot} = T_{\rm coh} + T_{\rm incoh}$. The incoherent part is calculated as $T_{\rm incoh} = (T_{\rm r}/(T_{\rm l} + T_{\rm r}))A$, herein $T_{\rm r}$ and $T_{\rm l}$ are the probabilities for right and left transmission from the region of inelastic scattering and A is the absorbed part which is given by $A = 1 - T_{\rm coh} - R_{\rm coh}$. This model, unlike Buttiker's model, describes dephasing that occurs throughout the system but still it has some major drawbacks in that it violates Onsager's two-terminal symmetry relations [6] and in the limit of strong absorption leads to perfect reflection.

Thus, there is a need for a model which is free from the shortcomings of the above two models. Brouwer and Beenakker [7] have developed a simple method, by mapping the three-probe Buttiker's method into a two-terminal geometry. This is done by eliminating the transmission coefficients which explicitly depend on the third probe by means of unitarity of the S-matrix. They consider a three-terminal geometry in which one of the probes is used as a voltage probe in the absence of magnetic flux (see the inset of figure 1). A current $I = I_1 = -I_2$ flows from the source to the drain. In this model, a fictitious third lead connects the ring to a reservoir at chemical potential μ_3 in such a way that no current is drawn, $(I_3 = 0)$. The 3×3 S-matrix of the entire system can be written as

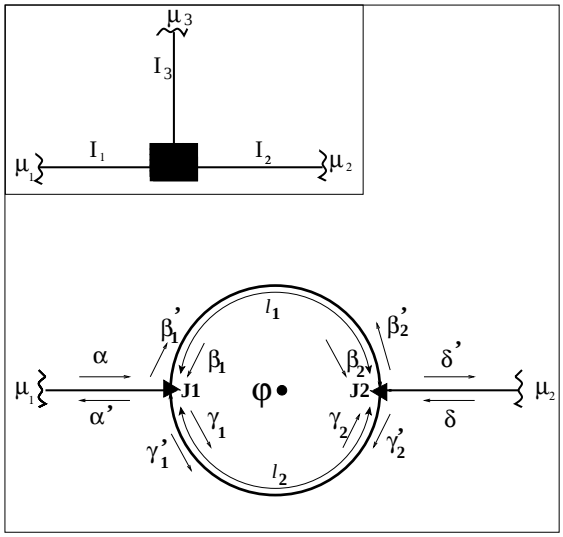

Figure 1. Aharonov–Bohm ring geometry. Inset shows the three-probe model.

$$S = \begin{pmatrix} r_{11} & t_{12} & t_{13} \\ t_{21} & r_{22} & t_{23} \\ t_{31} & t_{32} & r_{33} \end{pmatrix}.$$

Application of the relations [3,7,8] $I_p = \sum_q G_{pq}[\mu_p - \mu_q], p = 1,2,3$ and $G_{pq} = (2e^2/h)T_{pq}$ yields the (dimensionless) two-probe conductance $G = (h/2e^2)\,(I/(\mu_1 - \mu_2))$,

$$G = T_{21} + \frac{T_{23}T_{31}}{T_{31} + T_{32}}, \tag{1}$$

where $T_{pq} = T_{p \leftarrow q}$ is the transmission from qth to pth lead ($|t_{pq}|^2$). On elimination of the transmission coefficients in eq. (1) which involve the voltage probe, using the unitarity of the S-matrix, leads [7] to

$$G = T_{21} + \frac{(1 - R_{11} - T_{21})(1 - R_{22} - T_{21})}{1 - R_{11} - T_{21} + 1 - R_{22} - T_{12}}. \tag{2}$$

Now all the above coefficients are built from the 2×2 S-matrix

$$S' = \begin{pmatrix} r_{11} & t_{12} \\ t_{21} & r_{22} \end{pmatrix},$$

which represents the S-matrix of the absorbing system (non-hermitian) [9]. Thus re-injection has been reformulated in eq. (2). The first term in eq. (2) represents the conductance contribution from the phase coherent part. The second term accounts for electrons that are re-injected from the phase breaking reservoir, thereby ensuring particle conservation in the voltage-probe model. Also, eq. (2) restores Onsager's two-terminal symmetry relation for the optical potential model.

2.2 *Wave attenuation as a model for dephasing*

Though a major problem associated with the optical potential has been cured there still remains the problem that in the strong absorption limit it leads to perfect reflection, and absorption without reflection (spurious scattering) is not possible [10–12]. To overcome this problem, we, instead of making the Hamiltonian non-hermitian, add an exponential factor $e^{-\alpha l}$ to the S-matrix of the system. This is the model of wave attenuation. This describes dephasing which occurs throughout the system and removes the short comings of the optical potential model.

The wave attenuation model is not new. It has earlier been dealt with in the context of 1-D localization [10]. In the AB ring geometry considered here, the length of the upper arm is l_1 and that of lower arm is l_2 (see figure 1), and wave attenuation is inserted by the factor $e^{-\alpha l_1}$ (or $e^{-\alpha l_2}$) in the complex free propagator amplitudes, every time we traverse [8] the upper (or lower) arms of the ring. We have calculated the relevant transmission and reflection coefficients by using the S-matrix method along with the quantum wave guide theory for a single channel case. In this model, average absorption per unit length is given by 2α. With this method we show that the calculated conductance (G) in eq. (2) is symmetric under the flux reversal as required. The visibility of the AB oscillations rapidly decays as a function of α, indicating dephasing. Henceforth we refer to α as an incoherence parameter. Increasing α corresponds to increasing dephasing processes in the system or increase in temperature.

In figure 1, the total circumference of the loop is $L = l_1 + l_2$. The loop is connected to two current leads. The couplers (triangles) in figure 1 which connect the leads and the loop are described by a scattering matrix S. The S matrix for the left coupler yields the amplitudes $O_1 = (\alpha', \beta_1', \gamma_1')$ emanating from the coupler in terms of the incident waves $I_1 = (\alpha, \beta_1, \gamma_1)$, and for the right coupler yields the amplitudes $O_2 = (\delta', \beta_2', \gamma_2')$ emanating from the coupler in terms of the incident waves $I_2 = (\delta, \beta_2, \gamma_2)$. The S-matrix for either of the couplers [13] is given by

$$S = \begin{pmatrix} -(a+b) & \sqrt{\varepsilon} & \sqrt{\varepsilon} \\ \sqrt{\varepsilon} & a & b \\ \sqrt{\varepsilon} & b & a \end{pmatrix},$$

with $a = \frac{1}{2}(\sqrt{(1-2\varepsilon)} - 1)$ and $b = \frac{1}{2}(\sqrt{(1-2\varepsilon)} + 1)$. ε plays the role of a coupling parameter. The maximum coupling between the reservoir and the loop is $\varepsilon = \frac{1}{2}$, and for $\varepsilon = 0$, the coupler completely disconnects the loop from the reservoir.

The waves incident into the branches of the loop are related by the S matrices for upper branch by

$$\begin{pmatrix} \beta_1 \\ \beta_2 \end{pmatrix} = \begin{pmatrix} 0 & e^{ikl_1} e^{-\alpha l_1} e^{\frac{-i\theta l_1}{L}} \\ e^{ikl_1} e^{-\alpha l_1} e^{\frac{i\theta l_1}{L}} & 0 \end{pmatrix} \begin{pmatrix} \beta_1' \\ \beta_2' \end{pmatrix}$$

and, for the lower branch, by

$$\begin{pmatrix} \gamma_1 \\ \gamma_2 \end{pmatrix} = \begin{pmatrix} 0 & e^{ikl_2} e^{-\alpha l_2} e^{\frac{i\theta l_2}{L}} \\ e^{ikl_2} e^{-\alpha l_2} e^{\frac{-i\theta l_2}{L}} & 0 \end{pmatrix} \begin{pmatrix} \gamma_1' \\ \gamma_2' \end{pmatrix}.$$

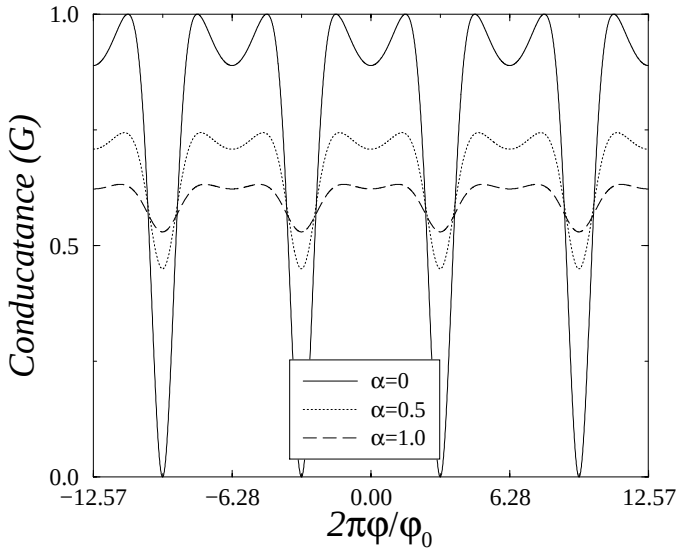

Figure 2. Reduction of Aharonov–Bohm oscillations in the presence of incoherence parameter α. $kL = \pi$, $l_1/L = 0.75$, $l_2/L = 0.25$, and coupling $\varepsilon = 0.5$.

These S-matrices of course are not unitary, $S(\alpha)S(\alpha)^\dagger \neq 1$, but they obey the relation $S(\alpha)S(-\alpha)^\dagger = 1$. The same relation is also obeyed by the S-matrix of the system in presence of an imaginary potential. Here kl_1 and kl_2 are the phase increments of the wave function in the absence of flux. $\theta l_1/L$ and $\theta l_2/L$ are the phase shifts due to flux in the upper and lower branches. Clearly, $(\theta l_1/L) + (\theta l_2/L) = 2\pi\Phi/\Phi_0$, where Φ is the flux piercing the loop and Φ_0 is the flux quantum hc/e. The transmission and reflection coefficients in eq. (2) are given as follows: $T_{21} = |\delta'/\alpha|^2$, $R_{11} = |\alpha'/\alpha|^2$, $R_{22} = |\delta'/\delta|^2$, $T_{12} = |\alpha'/\delta|^2$, where $\delta', \delta, \alpha', \alpha$ are as depicted in figure 1.

After calculating the required reflection and transmission coefficients we see that the coherent transmission T_{21} is not symmetric under the flux reversal. However, proper reinjection of carriers by eq. (2) for the total conductance G plotted in figure 2, shows that Onsager's symmetry relations are restored, i.e., G is symmetric under flux reversal. One notices from this figure that the amplitude of AB oscillations decreases with increase in incoherence parameter α. All parameters used in the following figures are in their dimensionless form.

In figure 3, we plot the visibility (V) as a function of the incoherence parameter α. The visibility is of course defined as

$$V = \frac{G_{\max} - G_{\min}}{G_{\max} + G_{\min}}. \tag{7}$$

The plot shows that with increase in the value of the parameter α the visibility exponentially falls off, reaching a point where it becomes zero corresponding to the disappearance of quantum interference effects, i.e., total dephasing in the system. In the inset of figure 3 we have plotted the first few Fourier [14] harmonics a_n ($n = 1$ to 4) of $G(\Phi)$ as a function of α. The harmonics are calculated using $a_n = \int_0^\pi G\cos(n\phi)\mathrm{d}\phi$. The harmonics

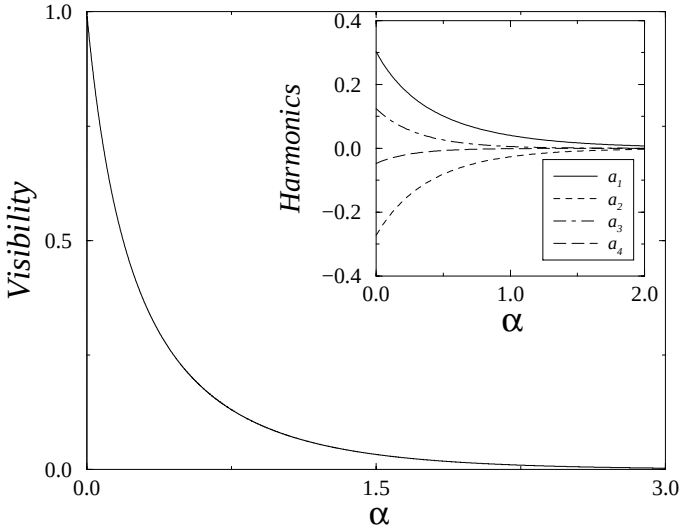

Figure 3. Visibility for the same physical parameters as in figure 2, coupling parameter $\varepsilon = 0.5$. In the inset the harmonics have been plotted for the same physical and coupling parameters.

exponentially fall off with increasing α with the exponent increasing as we go from 1 to 4. The *n*th-order harmonic corresponds to the contribution from the electronic paths which encircle the flux *n* times. The harmonics can sometimes show non-monotonic behavior depending on the physical parameters [15]. However, the visibility is a monotonic function of the incoherence parameter α.

Thus we have seen that wave attenuation can be effective in modeling absorption-induced dephasing in mesoscopic systems. In the next section we will see how this method is extended to measure the time a quantum particle takes to traverse a specified region of scattering.

3. Time in quantum mechanics

One of the most important problems in quantum mechanics is to calculate the time spent by a particle in a given region of space before scattering off from that region. The problem arises essentially due to the fact that there is no hermitian operator corresponding to this time in quantum mechanics [16–18]. The prospect of nanoscale electronic devices has in recent years brought new urgency to this problem as this is directly related to the maximum attainable speed of such devices. When it comes to tunneling time or time in general, there is a lot of ongoing controversy. In some formulations this time leads to a real quantity and in others to a complex quantity [19]. In certain cases tunneling time is considered to be ill-defined, i.e., quantum mechanics does not allow us to discuss this time [19–21]. Furthermore sometimes it is maintained that tunneling through a barrier takes zero time [22]. Recently, Anantha Ramakrishna and Kumar (AK) [23] have proposed the non-unitary optical potential as a clock to calculate the sojourn times without the clock affecting it.

In this paper we examine another non-unitary clock, viz., the attenuation of the wave to calculate the conditional lengths, i.e., the total effective distance traveled by a particle in the region of interest. This conditional length on appropriate division by the speed of the particle in the region of interest will give us the conditional time.

Any result for the time spent by a quantum particle in a given region of scattering should satisfy the criteria that (1) it should be real, (2) it should add up for non-overlapping regions, (3) it should be causally related to the interval of space, and (4) it should tend to the correct classical limits. It is shown explicitly by AK that all clock mechanisms involve spurious scattering, i.e., the very clock mechanism affects the sojourn times to be clocked finitely, even when the perturbation due to clock potential is infinitesimally small, as the perturbation due to clock mechanism couples to the Hamiltonian. This raises the question 'Can a quantum mechanical sojourn time be clocked with the clock affecting it?'. In this paper we introduce a method in which the perturbation is not introduced in the Hamiltonian but in the *S*-matrix of the system. In this case scattering is treated analogous to the Fabry–Perot interferometer. The scheme is illustrated in figure 4.

3.1 *Wave attenuation for the measurement of conditional times*

In the wave attenuation method [8,10], we damp the wave function by adding an exponential factor ($e^{-\alpha l}$) every time we traverse the length l of interest, here 2α represents the attenuation per unit length. This method is better than the optical potential model as it does not suffer from spurious scatterings [9,11,12]. The corrections introduced in case of the optical potential model to take care of spurious scatterings become manifestly difficult when we calculate the traversal times for a superlattice involving numerous scatterers. Thus our method of wave attenuation scores over the optical potential model. In the presence of wave attenuation a wave gets damped exponentially and thus the transmission (or reflection) coefficient changes exponentially with the length endured in the presence of the attenuator, and this acts as a natural counter for the sojourn lengths. Following the procedure of AK we calculate the traversal and reflection lengths and times in a given region of interest, in particular between two scatterers as in figure 4.

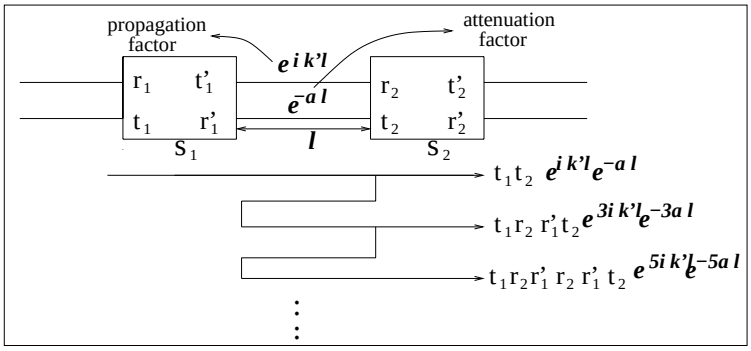

Figure 4. Summing the different paths, S_1 and S_2 denote the two scatterers. l is the distance between them. $e^{ik'l}$ and $e^{-\alpha l}$ denote the propagation and attenuation factors in the locality of interest.

The amplitude for transmission and reflection can be calculated by summing [8] the different paths as in figure 4. The scatterer S_1 in figure 1 has as its elements r_1, r_1', t_1 and t_1'. r_1 is the reflection amplitude when a particle is reflected from the left side of the barrier while r_1' is the reflection amplitude when a particle is reflected from the right side of the barrier. t_1 and t_1' are the amplitudes for transmission when a particle is transmitted from left to right of the barrier and vice-versa. Similar assignments are done for the scatterer S_2.

Thus for the amplitude of transmission we have $t = t_1 t_2 e^{ik'l} e^{-\alpha l} + t_1 r_2 r_1' t_2 e^{3ik'l} e^{-3\alpha l} + \cdots$ which can be summed as

$$t = \frac{t_1 t_2 e^{ik'l} e^{-\alpha l}}{1 - r_2 r_1' e^{2ik'l} e^{-2\alpha l}}, \tag{8}$$

and this is the transmission amplitude in the presence of wave attenuation. Again for the case of reflection amplitude we have $r = r_1 + t_1 r_2 t_1' e^{2ik'l} e^{-2\alpha l} + t_1 r_2 r_1' r_2 t_1' e^{4ik'l} e^{-4\alpha l} + t_1 r_2 r_1' r_2 r_1' r_2 t_1' e^{6ik'l} e^{-6\alpha l} + \cdots$, which leads to

$$r = \frac{r_1 - a r_2 e^{2ik'l} e^{-2\alpha l}}{1 - r_1' r_2 e^{2ik'l} e^{-2\alpha l}}. \tag{9}$$

In eq. (5), $a = r_1 r_1' - t_1 t_1'$ is the determinant of the S-matrix of the first barrier, and as we are only dealing with unitary S-matrices, the determinant is of unit modulus for all barriers. In these expressions k' is the wave vector in the region of interest. The transmission and reflection coefficients can be calculated by taking the square of the modulus of the expressions in eqs (4) and (5).

The traversal length for transmission is calculated as below [23]:

$$l^{\mathrm{T}} = \lim_{2\alpha \to 0} - \frac{\partial(\ln |t|^2)}{\partial(2\alpha)}, \tag{10}$$

and the reflection length in case of reflection is defined as

$$l^{\mathrm{R}} = \lim_{2\alpha \to 0} - \frac{\partial(\ln |r|^2)}{\partial(2\alpha)}. \tag{11}$$

The traversal times for transmission, or the reflection times in case of reflection, can be calculated using $\tau^{\mathrm{R/T}} = l^{\mathrm{R/T}}/(\hbar k'/m)$, where, as before, $\hbar k'/m$ is the speed of propagation in the region of interest. For the case of the potential profile sketched in figure 5, $k' = k$. From eqs (6) and (7) we can calculate the traversal length for transmission

$$\frac{l^{\mathrm{T}}}{l} = \frac{1 - |r_1'|^2 |r_2|^2}{1 - 2\Re(r_1' r_2 e^{2ik'l}) + |r_1'|^2 |r_2|^2} \tag{12}$$

and for reflection,

$$\frac{l^{\mathrm{R}}}{l} = \frac{l^{\mathrm{T}}}{l} + \frac{|r_2|^2 - |r_1|^2}{|r_1|^2 - 2\Re(r_1^* r_2 a e^{2ik'l}) + |r_2|^2}. \tag{13}$$

Here $\Re$ represents the real part of the quantity in brackets. In the above two equations the traversal and reflection lengths have been normalized with respect to the length l of the

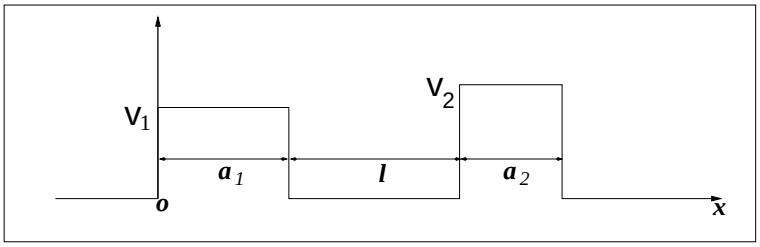

Figure 5. The double heterostructure. Barriers are denoted by their width a_j and height V_j, $j = 1, 2$. The width of the well is l.

locality of interest, which is the width of the well region of the potential profile of figure 5. Throughout the discussion the quantities are expressed in their dimensionless form.

We consider the case of two rectangular barriers as shown in figure 5 separated by a distance l. The energies, potentials and the lengths are all in their dimensionless form.

The S-matrices for the double heterostructure are given as

$$S_j = \begin{pmatrix} r_j & t'_j \\ t_j & r'_j \end{pmatrix} = \begin{pmatrix} \frac{-i\varepsilon_{j+}\sinh K_j a_j}{2\cosh K_j a_j - i\varepsilon_{j-}\sinh K_j a_j} & \frac{2e^{-ika_j}}{2\cosh K_j a_j - i\varepsilon_{j-}\sinh K_j a_j} \\ \frac{2e^{-ika_j}}{2\cosh K_j a_j - i\varepsilon_{j-}\sinh K_j a_j} & \frac{-e^{-2ika_j} i\varepsilon_{j+}\sinh K_j a_j}{2\cosh K_j a_j - i\varepsilon_{j-}\sinh K_j a_j} \end{pmatrix},$$

where $K_j = \sqrt{(2m(V_j - E))/\hbar^2}$, $k = \sqrt{2mE/\hbar^2}$ and $\varepsilon_{j\pm} = (k/K_j) \pm (K_j/k)$, $j = 1, 2$.

In figure 6 we have plotted the transmission coefficient and the normalized times τ^{T} ($=\tau^{\mathrm{R}}$) for a symmetrical double barrier $V = V_1 = V_2$. These times are those required by a quantum particle to traverse or reflect from the well of the double heterostructure. We have normalized these times by the time $ml/\hbar k'$ taken by a particle to traverse the length l, without the potential profile shown in figure 5. From eq. (8), it is clear that the transmission time is always positive. Moreover, we can readily show from our treatment that the local times spent by the particle in non-overlapping regions are additive. As expected the traversal times are larger near the resonances. In case of non-symmetrical structures one obtains negative reflection times (which should not be surprising) in some parameter region but traversal times are positive for both symmetrical as well as non-symmetrical structures. It can be argued [23] that this is because in case of reflection there is a partial wave corresponding to prompt reflection r_1 that never samples the region of interest, and also this prompt part leads to self interference delays which cause the sojourn time τ^{R} to become negative for some values of the parameters. If one removes this prompt part, i.e., $r_{np} = r - r_1$, and we re-calculate the sojourn time $\tau^{\mathrm{R}_{np}}$ with this prompt part removed, we find it to be positive and given by $\tau^{\mathrm{R}_{np}} = \tau^{\mathrm{T}} + 1$, τ^{T} is positive. In the case of non-symmetrical structures τ^{T} is independent of whether a particle is incident from the left or the right, but τ^{R} depends on the direction of the incident particle. There is also a remarkable assertion found in the literature [17] concerning the measurement of the time of transmission or reflection, which is $\tau^{\mathrm{D}} = T\tau^{\mathrm{T}} + R\tau^{\mathrm{R}}$. Herein τ^{T} and τ^{R} are as given above while the dwell time is $\tau^{\mathrm{D}} = \frac{1}{v}\int_0^l |\psi|^2 \mathrm{d}x$. ψ is the wave function in the locality of interest and v is the speed of the particle in the region of interest. We have verified by explicit calculation that this equivalence does not hold [16,24]. Our method can also be

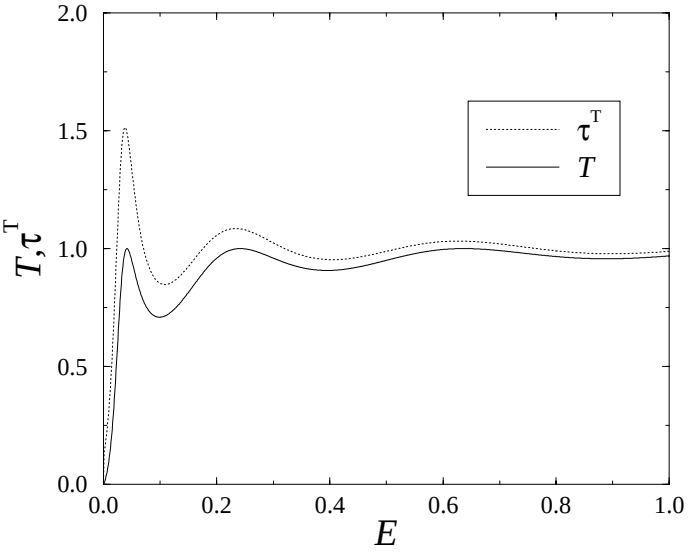

Figure 6. T and τ^{T} for a symmetric double heterostructure. $l = 10.0$, $V_1 = V_2 = 1.0$ and $a_1 = a_2 = 0.2$.

readily extended to the calculation of traversal time of tunneling (for the case of a single barrier). The results are in agreement with recent calculations [23].

4. Conclusion

In conclusion, we have shown that the method of wave attenuation works much better in modeling dephasing due to absorption than its counterpart, the optical potential. When we extend this method to calculate the conditional sojourn times, we find here also wave attenuation is easier to deal with than optical potential.

References

[1] Y Imry, *Introduction to mesoscopic physics* (Oxford University Press, New York, 1997)
[2] Florian Marquardt, *An introduction to the basics of dephasing*, http://iff.physik.unibas.ch/ florian/dephasing/dephasing.html
[3] M Buttiker, *Phys. Rev.* **B33**, 3020 (1986); *IBM J. Res. Dev.* **32**, 63 (1988)
[4] Y Zohta and H Ezawa, *J. Appl. Phys.* **72**, 3584 (1992)
[5] Hu Yuming, *J. Phys.* **C21**, L23 (1988)
[6] T P Pareek, Sandeep K Joshi, and A M Jayannavar, *Phys. Rev.* **B57**, 8809 (1998)
[7] P W Brouwer and C W J Beenakker, *Phys. Rev.* **B55**, 4695 (1997)
P W Brouwer, Ph.D. thesis (Insttuut-Lorentz, University of Leiden, The Netherlands, 1997)
[8] S Datta, *Electron transport in mesoscopic systems* (Cambridge University Press, Cambridge, 1995)

[9] Colin Benjamin and A M Jayannavar, *Phys. Rev.* **B65**, 153309 (2002) preprint cond-mat/0112153
[10] Sandeep K Joshi, D Sahoo and A M Jayannavar, *Phys. Rev.* **B62**, 880 (2000)
P Pradhan, preprint cond-mat/9807312
[11] A M Jayannavar, *Phys. Rev.* **B49**, 14718 (1994)
A K Gupta and A M Jayannavar, *Phys. Rev.* **B52**, 4156 (1995)
[12] A Rubio and N Kumar, *Phys. Rev.* **B47**, 2420 (1993)
[13] M Buttiker, Y Imry and M Ya Azbel, *Phys. Rev.* **A30**, 1982 (1984)
[14] J B Xia, *Phys. Rev.* **B45**, 3593 (1992)
[15] S K Joshi, D Sahoo and A M Jayannavar, *Phys. Rev.* **B64**, 075320 (2001)
[16] R Landauer and Th Martin, *Rev. Mod. Phys.* **66**, 217 (1994)
[17] E Hauge and J A Stovneng, *Rev. Mod. Phys.* **61**, 917 (1989)
[18] V Gasparian, M Ortuno, G Schon and U Simon, *Tunneling time in nanostructures*, http://bohr.fcu.um.es/papers/1999/gasparian.pdf
[19] D Sokolovski and L M Baskin, *Phys. Rev.* **A36**, 4604 (1987)
[20] N Yamada, *Phys. Rev. Lett.* **83**, 3350 (1999)
[21] A Steinberg, *Phys. Rev. Lett.* **74**, 2405 (1995)
[22] E O Kane, in *Tunneling phenomena in solids* edited by E Burstein and S Lundquist (Plenum, New York, 1969) p. 1
[23] S Anantha Ramakrishna and N Kumar, preprint cond-mat/0009269
S Anantha Ramakrishna, Ph.D. Thesis (Raman Research Institute, Bangalore, India, 2001)
[24] Colin Benjamin and A M Jayannavar, *Solid State Comm.* **121**, 591 (2002) preprint cond-mat/0112499